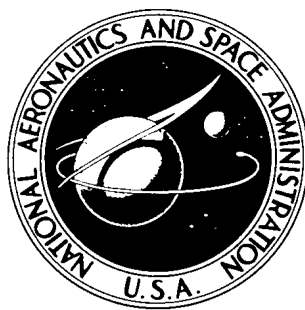


NASA TECHNICAL NOTE



NASA TN D-3830

NASA TN D-3830

FLIGHT DEMONSTRATION OF A SKIN-FRICTION GAGE TO A LOCAL MACH NUMBER OF 4.9

by Darwin J. Garringer and Edwin J. Saltzman

Flight Research Center

Edwards, Calif.

FLIGHT DEMONSTRATION OF A SKIN-FRICTION GAGE
TO A LOCAL MACH NUMBER OF 4.9

By Darwin J. Garringer and Edwin J. Saltzman

Flight Research Center
Edwards, Calif.

NATIONAL AERONAUTICS AND SPACE ADMINISTRATION

For sale by the Clearinghouse for Federal Scientific and Technical Information
Springfield, Virginia 22151 - Price \$1.00

FLIGHT DEMONSTRATION OF A SKIN-FRICTION GAGE TO A LOCAL MACH NUMBER OF 4.9

By Darwin J. Garringer and Edwin J. Saltzman
Flight Research Center

SUMMARY

A small, commercially available skin-friction gage was flight tested on the X-15 airplane. The Reynolds number range investigated extended from 3.3×10^6 to 8.0×10^6 , and local Mach numbers ranged from 0.7 to 4.9. The ratio of wall-to-recovery temperature varied from about 0.4 to 1.4.

The gage, its cooling system, and the supporting instrumentation performed well. Turbulent skin-friction values measured in flight for a wide range of wall-to-recovery temperature ratios are similar in level to adiabatic flat-plate wind-tunnel results for corresponding Mach numbers and Reynolds numbers. Thus, for the present tests the influence of wall-to-recovery temperature ratio appears to be less than estimated by turbulent theory.

INTRODUCTION

The ability to predict skin-friction drag and associated aerodynamic heating is of major importance in the design of large, high-speed, long-range aircraft such as supersonic or hypersonic transports. The skin-friction drag may be as much as 30 percent to 35 percent of the total drag at a Mach number near 3, thus the ability to accurately predict the full-scale performance of the vehicle will depend largely on the ability to predict skin-friction drag.

At present, it is not possible to formulate a complete method for predicting compressible, turbulent skin friction without empirical constants. Wind-tunnel data are generally used to establish the empirical constants, but a wind tunnel cannot simulate simultaneously all the parameters experienced in full-scale flight. Therefore, the NASA Flight Research Center, at Edwards, Calif., initiated several full-scale flight experiments to augment wind-tunnel investigations by other experimenters.

Skin friction can be measured relatively simply and directly with a force balance type of instrument, usually referred to as a skin-friction gage. Skin-friction gages of sufficient sensitivity have had a tendency to be too bulky for use in flight if made durable enough to withstand the flight environment. Recently, however, gages have been developed that are compact and rugged yet sensitive. This paper describes an investigation in which one of these gages was used in the relatively harsh environment

imposed by flight at free-stream Mach numbers up to 5.5 (local Mach numbers to 4.9). Data from two flights are presented in the form of the ratio of measured skin-friction coefficient to theoretical, incompressible, turbulent skin-friction coefficient as a function of Mach number. These data are compared with wind-tunnel results and theory.

SYMBOLS

Physical quantities are presented, where applicable, in both U. S. Customary Units and the International System of Units (SI). Factors relating the systems are given in reference 1.

A	area of floating element, ft^2 (cm^2)
C_{F_i}	average incompressible, turbulent skin-friction coefficient
C_f	measured skin-friction coefficient, $\frac{\tau}{q_l}$
C_{f_i}	local, incompressible, turbulent skin-friction coefficient
F	shearing force measured by skin-friction gage, lb (mg)
M_l	local Mach number
M_∞	free-stream Mach number of airplane
p_l	local static pressure from static-pressure orifice on test panel, lb/ft^2 (N/m^2)
q_l	local free-stream dynamic pressure, $0.7 M_l^2 p_l$, lb/ft^2 (N/m^2)
R	Reynolds number
r	turbulent recovery factor, 0.89
T	temperature, $^\circ\text{F}$ ($^\circ\text{C}$) and $^\circ\text{R}$
T_l	local free-stream temperature, $^\circ\text{F}$ and $^\circ\text{R}$ ($^\circ\text{C}$ and $^\circ\text{K}$)
T_r	recovery temperature, $T_l(1 + 0.2r M_l^2)$, $^\circ\text{R}$ ($^\circ\text{K}$)
T_t	total temperature, $^\circ\text{R}$ ($^\circ\text{K}$)
T_w	temperature of skin measured by thermocouple, $^\circ\text{F}$ ($^\circ\text{C}$) and $^\circ\text{R}$

T_{∞}	ambient temperature, °F and °R (°C and °K)
Δ	error
τ	shearing stress on floating element of gage, $\frac{F}{A}$, lb/ft ² (mg/cm ²)

TEST FACILITY

The high supersonic velocities required for this study were obtained by installing the experiment on the X-15 airplane. The X-15 is a single-place, low-aspect-ratio monoplane designed for manned flight research to a Mach number near 6. A three-view drawing and a photograph of the X-15 are shown in figures 1 and 2, respectively. A more detailed description of the airplane and its capabilities is presented in reference 2.

The experiment was installed on the movable portion of the X-15 upper vertical fin. Originally, the leading edge of the fin was blunt, in consideration of structural heating associated with high supersonic flight. Prior to this study, however, the leading edge of the movable portion of the fin was modified from an original diameter of 1 inch (2.54 centimeters) to about 0.03 inch (0.76 millimeter). This change avoided the effects of a shock-induced shear layer being superimposed over the viscous boundary layer. In addition, the sharper leading edge more nearly approaches the flat-plate configurations commonly used in wind-tunnel friction studies, thus making comparison of these flight data with results from such facilities more meaningful.

A photograph of the upper movable vertical fin with the modified leading edge is shown in figure 3, and a sketch is presented in figure 4.

A known minimum length of turbulent flow was established by tripping the boundary layer. The boundary-layer trips consisted of small drops of welding material approximately 0.1 inch (2.5 millimeters) in diameter, 0.02 inch (0.5 millimeter) high, and 1.0 inch (25 millimeters) apart. The trips were placed in a row parallel to and approximately 4.8 inches (12.2 centimeters) aft of the leading edge (fig. 4).

INSTRUMENTATION

General Description

A boundary-layer rake, thermocouples, and flush surface orifices to measure local flow parameters were installed with a skin-friction gage on the upper vertical fin of the X-15 airplane. Data from these sensors were recorded within the aircraft. Pressures were recorded by standard NASA 12-cell photorecording manometers. The skin-friction-gage output voltage and thermocouple temperatures were recorded by oscillographs. Data were synchronized by a timer common to all the recording instruments. Figure 5 is a closeup view of the instrument installation.

The location of the instruments on the fin and the geometry of the fin are shown in figure 4. The individual instruments are described in the following paragraphs.

Skin-Friction Gage

Description. — The skin-friction gage investigated was a commercially developed, liquid-cooled force balance. The specifications and dimensions of the gage are given in table I. The flush circular surface referred to as a "floating element" in the center of the top of the gage is mounted on small wire flexures and held centered by electromagnets. Any force that attempts to displace the floating element along the sensitive axis of the gage causes a change in voltage to the electromagnets. Thus, a restoring electromagnetic force is produced that balances the force which is attempting to displace the floating element. The value of the shearing force caused by the friction of air flowing over the gage is obtained by measuring the voltage necessary to produce the restoring force. The relationship of the voltage to the restoring force was determined from between-flight calibrations. The calibrations were made by hanging small weights from the floating element and measuring the output voltage while the sensitive axis was aligned vertically.

The floating element of the skin-friction gage did not protrude above and was less than 0.0005 inch (0.0127 millimeter) below the surrounding surface at room temperature. A study described in reference 3 indicates that effects of such a small displacement produce force values between 1 and 2 percent low. The space around the floating element (gap between the floating element and the rest of the gage) was uniform and was less than 0.001 inch (0.0254 millimeter) when power was applied to the gage.

The top surface of the gage was mounted flush (within ± 0.001 in. (0.0254 mm)) with the surface of the panel in which the gage was mounted. This panel was flush, within ± 0.001 inch (0.0254 millimeter), with the adjacent skin of the aircraft. The heads of the screws in front of the gage were filled in, then ground smooth for the two flights discussed herein.

Checkout and calibration. — The skin-friction gage was subjected to extensive laboratory testing under transient and constant temperature conditions before it was used in flight. The transient-temperature test consisted of hanging known weights on the floating element with the sensitive axis aligned vertically, then subjecting the surface of the gage and the surrounding skin to radiant heating which was programmed to vary from room temperature to 1000° F (538° C). This programming simulated the skin temperature history that was expected at the test location during the two flights of this study.

The results of the transient temperature test showed that the cooling system was adequate and that the gage would function under these conditions. Additional details pertaining to the cooling system are given in the appendix.

The constant-temperature test was performed at the following temperature levels: -70, -35, 0, 74, 130, and 200° F (-57, -37, -18, 23, 54, and 93° C). The test environment was maintained at a constant temperature until the temperature of the entire gage was the same as that of the environment. Weights were then suspended from the floating element through the use of a small wire hanger while the sensitive

axis was alined vertically as for the transient temperature tests. The output voltage of the gage was then recorded. Figure 6(a) is a plot of the data from a constant-temperature test made before the transient-temperature tests. Figure 6(b) is data from a similar constant-temperature test performed after the transient-temperature test. Comparison of the two figures indicates a significant reduction in the effects of temperature following the transient temperature test, that is, repeated cycling (room temperature to 1000° F (538° C) during the transient-temperature tests greatly reduced the sensitivity of the gage to temperature. A technical explanation of this effect is beyond the scope of this paper. The results of another constant-temperature test performed after the flight tests agreed with the results of figure 6(b), thus it was considered unnecessary to apply adjustments to the gage output for temperature effects.

During the constant-temperature test it was noticed that a shift in calibration, due to a change in the zero-load output voltage, occurred between tests. Consequently, preflight and postflight checks were made for each flight to provide the correct calibration intercept for each flight and to verify that the preflight and postflight calibration slopes were the same. Intercept shifts in calibration were noticed between flights, but preflight and postflight intercepts for a given flight were always in agreement.

Boundary-Layer Rake

The stagnation pressure obtained from the top probe of the boundary-layer rake was used with the static pressure obtained from the orifice in the test panel to obtain local Mach number immediately outside the boundary layer at the rake location. A boundary-layer rake of this same basic design was calibrated in the NASA Langley Research Center's 4- by 4-foot (1.22- by 1.22-meter) supersonic pressure tunnel at Mach numbers of 4 and 4.7. At these Mach numbers, the calibration indicated that the probes used in this investigation were free of any interference from the rake strut or adjacent probes.

Thermocouples

The thermocouples used in this study were the same type as used in the heat-transfer study of reference 4. Thermocouples were placed on the cooling jacket and the body of the gage, on the gage mounting plate, and on the skin of the fin approximately 3 inches (7.6 centimeters) in front of the gage. The latter thermocouple was used to measure wall temperature.

DATA-REDUCTION PROCEDURE

The shearing force measured by the skin-friction gage was reduced to skin-friction coefficients by using the following equation:

$$C_f = \frac{F}{q_l A} = \frac{\tau}{q_l}$$

In order to present the skin-friction coefficient as a function of one parameter, local Mach number, the experimentally obtained coefficient was divided by the theoretical, incompressible, turbulent skin-friction coefficient obtained from the Karman-Schoenherr equation (refs. 5 and 6):

$$C_{f_i} = \frac{0.242 C_{F_i}}{0.242 + 0.8686 \sqrt{C_{F_i}}}$$

The average incompressible skin-friction coefficient C_{F_i} is related to Reynolds number as follows:

$$\frac{0.242}{\sqrt{C_{F_i}}} = \log(C_{F_i} R) \text{ (ref. 7).}$$

Reynolds number was based on local conditions and the distance from the boundary-layer trips to the center of the gage.

Local Mach number was obtained by applying the Rayleigh pitot relationship to the measured stagnation pressure obtained from the top probe of the rake and static pressure obtained from the flush orifice. Total temperature was calculated from the relationship $T_t = T_\infty(1 + 0.2M_\infty^2)$, where the ambient temperature at the altitude of the aircraft was obtained from radiosonde data. The total temperature was assumed to be constant throughout the flow, and the local Mach number was used to obtain local free-stream temperature as follows:

$$T_l = \frac{T_\infty (1 + 0.2M_\infty^2)}{(1 + 0.2M_l^2)}$$

Local free-stream temperature was, in turn, used to calculate Reynolds number and recovery temperature.

RELIABILITY AND ERROR

Limitations imposed on the X-15 trajectory by minimum thrust and occasional fuel-line cavitation determine the portions of a flight in which quasi-steady aerodynamic conditions can be achieved. For this study the attainment of relatively steady reference conditions along with dynamic pressures of 1000 lb/ft² (48,000 N/m²) or greater is important to prevent lag from influencing the calculated values of local dynamic pressure.

The results of this study above $M_\infty \approx 3$ meet the requirement of relatively high dynamic pressure, and the data obtained near peak Mach numbers represent relatively low rates of change of dynamic pressure. Thus, near maximum Mach number for each of the flights and/or at dynamic pressures significantly above 1000 lb/ft² (48,000 N/m²) the data are believed to be unaffected by lag. When present at lower

Mach numbers, lag would tend to produce values of $\frac{C_f}{C_{f_i}}$ that would be too high when dynamic pressure is increasing and too low when dynamic pressure is decreasing.

Another factor that should be mentioned is the possible, though small, effect of the tip and root of the movable portion of the vertical fin on the test results. The respective Mach lines sweep in front of the test complex below Mach numbers of 2 and 3, thus only results at Mach numbers above 3 may be considered to be free of tip and root effects. Although the effect of the discontinuity in the leading-edge line of the movable portion of the fin is believed to be negligible, theoretically, the Mach line is always in front of the test panel for the conditions of this study.

Because the floating element and the surrounding material have different heat capacities per unit of surface area, they will present a surface temperature discontinuity to the oncoming boundary-layer flow. Such a discontinuity can influence the heat transfer from a fluid to a body, thus one may suspect that such a discontinuity may affect resultant skin-friction values. It is not known whether the surface temperature discontinuity is significant for the present study; however, it was indicated in reference 8 that for temperature differences up to 56° F (31° C) the resultant discontinuity effect, if any, was less than 2 percent.

Bias Errors

The data of this study for Mach numbers greater than 3.5 are believed to contain bias errors that cause the results, as presented, to be as much as 3 percent low. The reasons for possible bias are: (1) possible depression of the floating element which would make C_f too low¹ (also noted in the section entitled Skin-Friction Gage), (2) expansion of the floating element so that the exposed area, as measured at room temperature, is too small, resulting in calculated C_f being too high, and (3) uncertainty of the exact location of the virtual origin of turbulence which would cause C_{f_i} to be calculated too high.

Additional bias can occur at Mach numbers below about 3.5 because of possible lag effects, and below Mach numbers of 2 and 3, respectively, small tip and root effects may be present, as previously mentioned.

Random Errors

Errors that are considered random or for which the direction of bias is unknown, such as in determining the area of the floating element at room temperature, are listed in the following tabulation with the estimated effects on friction coefficients:

¹At present, there is no absolute proof whether the level of the element with respect to the surrounding surface is affected by temperature.

Error source	$\frac{\Delta C_f}{C_f}$, percent	Error source	$\frac{\Delta C_{f_i}}{C_{f_i}}$, percent
Friction balance output	±4	Stagnation pressure	±1
Area of floating element	±1	Static pressure	±1
Dynamic pressure	±2	Temperature	±2

To summarize, for Mach numbers of 3.5 and above the absolute standard deviation is believed to be between ±5 percent and ±6 percent with a possible bias of about -3 percent.

TEST CONDITIONS

Local dynamic pressure varied from approximately 250 lb/ft² (12,000 N/m²) to about 2100 lb/ft² (100,600 N/m²). Zero or negligible sideslip angles were maintained throughout the test flights; however, angle-of-attack excursions were significant. The present analysis excludes results when angles of attack exceeded about 3° (0.052 rad) so that the aircraft canopy and other upstream parts would not interfere with the flow over the experiment.

Reynolds number, based on local flow conditions and the distance between the friction gage and boundary-layer trips, varied between 3.3×10^6 and 8.0×10^6 . Data are presented for local Mach numbers from 0.7 to 4.9 and wall-to-recovery temperature ratios between 0.4 and 1.4.

DISCUSSION

Presentation of Data

Results obtained from two X-15 flights (referred to as A and B) are presented in figure 7(a) in the form of the ratio of compressible to incompressible local turbulent skin-friction coefficients plotted as a function of local Mach number. Included with the flight data are theoretical curves of these same parameters for three values of wall-to-recovery temperature ratio. The theoretical values of the compressible skin-friction coefficient C_f are derived from the reference temperature method of

Sommer and Short (refs. 5, 9, and 10). The theoretical incompressible values are those of the Karman-Schoenherr equation, which was also the denominator used with the flight results.

The solid and dashed curves in figure 7(b) show the approximate values of wall-to-recovery temperature ratio for each of the two flights. It is believed that the relatively low values of $\frac{C_f}{C_{f_i}}$ for decelerating flight below a Mach number of about 3.5 on flight B result, in part, from lag effects on calculated dynamic pressure (see RELIABILITY AND ERROR section). The relatively wide range in $\frac{T_w}{T_r}$ covered

during each flight relative to the dispersion of data points (fig. 7(a)) would suggest that the importance of the ratio of wall-to-recovery temperature is somewhat over-estimated by the theory. This result agrees with the results of heat-transfer studies on the X-15 airplane (refs. 11 and 12) and a preliminary assessment of the present X-15 skin-friction experiment included in reference 12.

The variation with time of local dynamic pressure, local Mach number, and wall temperature for each of the flights is shown in figure 8.

Comparison With Other Experiments

The results of this experiment are compared in figure 9 with experimental results from several wind-tunnel facilities (refs. 10 and 13 to 16). All of the wind-tunnel data were obtained by using skin-friction gages on either flat plates with sharp leading edges or a flat tunnel wall, although none of the gages were of the same type as used in the present experiment. The wall-to-recovery temperature ratios were near unity for all of the wind-tunnel data; whereas, the flight temperature ratio varied from 0.4 to 1.4. In spite of these differences in wall-to-recovery temperature ratios, the data of the present flight study and the wind-tunnel results have similar levels of friction ratio $\frac{C_f}{C_{fi}}$ for corresponding Mach numbers and Reynolds numbers.

CONCLUSIONS

A study of the feasibility of using a small, commercially available skin-friction gage in the environment generated by X-15 flight to a local Mach number of 4.9 led to the following conclusions:

1. The gage, its cooling system, and supporting instrumentation performed well.
2. Turbulent skin-friction values measured in flight for a wide range of wall-to-recovery temperature ratios are similar in level to adiabatic flat-plate wind-tunnel results for corresponding Mach numbers and Reynolds numbers. Thus, for the tests of this study the influence of wall-to-recovery temperature ratio appears to be less than estimated by theory.

Flight Research Center,
National Aeronautics and Space Administration,
Edwards, Calif., November 10, 1966
719-01-00-03-24

APPENDIX

THE COOLING SYSTEM

The vital working parts of the skin-friction gage investigated must be maintained at temperatures not to exceed 212° F (100° C). A design feature of the gage is the threaded retaining nut which secures the device to the mounting plate. This nut is a hollow chamber and acts as a cooling jacket through which a coolant may flow (table I).

William P. Albrecht of the NASA Flight Research Center, Flight Operations Division, designed a pressure-energized coolant delivery system to provide the required coolant flow. This system is shown schematically in figure 10, and a photograph is presented in figure 11.

The coolant vessel was serviced with a solution of three parts ethylene glycol (standard permanent automobile antifreeze) with two parts of water, by volume. This vessel was filled to the overflow level, about 44 ounces (1250 grams), then capped. With the solenoid valve closed, the pressure vessel was serviced before each flight with gaseous nitrogen. A 15-psi (103,421-N/m²) relief valve maintained a near-constant differential pressure (between vessel and ambient) as the X-15 was carried to launch altitude prior to use of the cooling system.

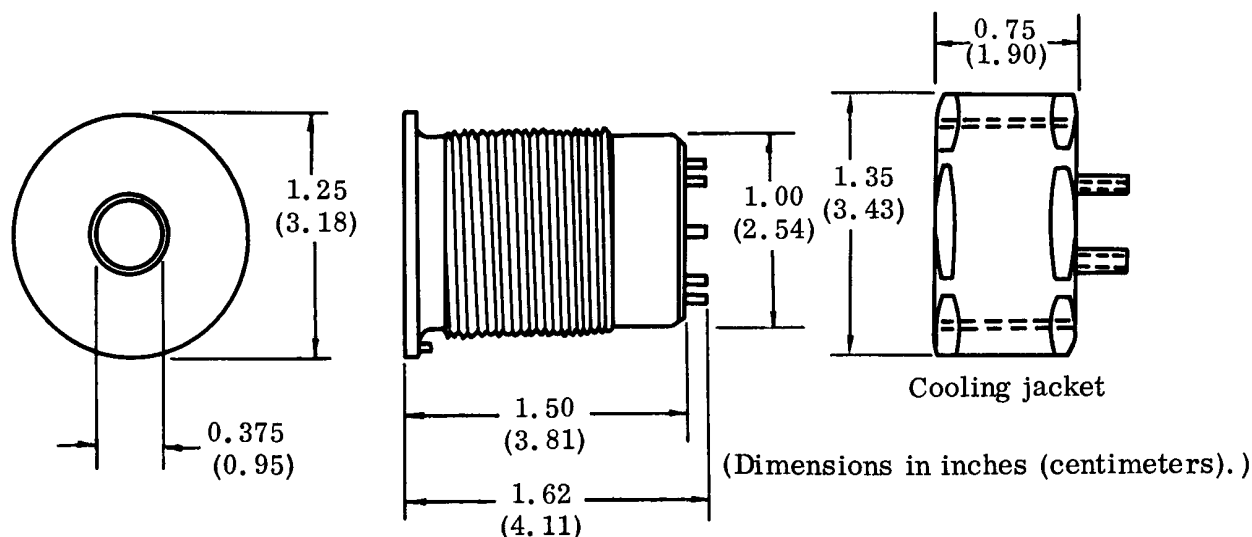
About 1 minute before the X-15 was launched from the B-52 carrier airplane, the pilot activated the solenoid valve which caused coolant to flow through the cooling jacket and thence overboard. The combination of up to 15-psi (103,421-N/m²) pressure head on the fluid and the 0.031-inch (0.787-millimeter) diameter orifice provided coolant flow throughout the heating portion of the flights. The pilot usually closed the solenoid valve as he neared the landing site, after from 5 to 7 minutes of operation. Although detailed records were not kept of the amount of coolant used, it was observed that usage varied between one third and two thirds of capacity. The coolant flow was thus adequate, and a significant margin of safety existed. Figure 12 illustrates the effectiveness of the cooling system in keeping the gage temperatures below the maximum permissible level while wall temperatures nearby were approaching 900° F (482° C). Figure 12(a) shows the location of several thermocouples used to sense temperatures that are plotted in history form in figure 12(b). Note that the main body and electronic components of the gage never exceeded 140° F (60° C). The temperature of the floating element was not measured because of technical difficulties involved in achieving such a measurement without affecting the observed values of shear stress.

REFERENCES

1. Mechtly, E. A. : The International System of Units - Physical Constants and Conversion Factors. NASA SP-7012, 1964.
2. Weil, Joseph: Review of the X-15 Program. NASA TN D-1278, 1962.
3. O'Donnell, Francis B., Jr. : A Study of the Effect of Floating-Element Misalignment on Skin-Friction-Balance Accuracy. Rep. DRL 515, CR-10, Defense Res. Lab., Univ. of Texas, Mar. 5, 1964.
4. Banas, Ronald P. : Comparison of Measured and Calculated Turbulent Heat Transfer in a Uniform and Nonuniform Flow Field on the X-15 Upper Vertical Fin at Mach Numbers of 4.2 and 5.3. NASA TM X-1136, 1965.
5. Peterson, John B., Jr. : A Comparison of Experimental and Theoretical Results for the Compressible Turbulent-Boundary-Layer Skin Friction With Zero Pressure Gradient. NASA TN D-1795, 1963.
6. Bertram, Mitchel H. : Calculations of Compressible Average Turbulent Skin Friction. NASA TR R-123, 1962.
7. Locke, F. W. S., Jr. : Recommended Definition of Turbulent Friction in Incompressible Fluids. DR Rept. No. 1415, Navy Dept., Bur. of Aeronautics, Res. Div., June 1952.
8. Westkaemper, John C. : Step-Temperature Effects on Direct Measurements of Drag. AIAA J., vol. 1, no. 7, July 1963, pp. 1708-1710.
9. Sommer, Simon C.; and Short, Barbara J. : Free-Flight Measurements of Turbulent-Boundary-Layer Skin Friction in the Presence of Severe Aerodynamic Heating at Mach Numbers From 2.8 to 7.0. NACA TN 3391, 1955.
10. Hopkins, Edward J.; and Keener, Earl R. : Study of Surface Pitots for Measuring Turbulent Skin Friction at Supersonic Mach Numbers — Adiabatic Wall. NASA TN D-3478, 1966.
11. Quinn, Robert D.; and Kuhl, Albert E. : Comparison of Flight-Measured and Calculated Turbulent Heat Transfer on the X-15 Airplane at Mach Numbers From 2.5 to 6.0 at Low Angles of Attack. NASA TM X-939, 1964.
12. Banner, Richard D.; and Kuhl, Albert E. : A Summary of X-15 Heat-Transfer and Skin-Friction Measurements. NASA TM X-1210, 1966.
13. Matting, Fred W.; Chapman, Dean R.; Nyholm, Jack R.; and Thomas, Andrew G. : Turbulent Skin Friction at High Mach Numbers and Reynolds Numbers in Air and Helium. NASA TR R-82, 1961.

14. Coles, Donald: Measurements in the Boundary Layer on a Smooth Flat Plate in Supersonic Flow - III. Measurements in a Flat-Plate Boundary Layer at the Jet Propulsion Laboratory. Rep. No. 20-71, Jet Prop. Lab., Calif. Inst. Tech., June 1, 1953.
15. Moore, D. R.; and Harkness, J.: Experimental Investigations of the Compressible Turbulent Boundary Layer at Very High Reynolds Numbers. AIAA J., vol. 3, no. 4, Apr. 1965, pp. 631-638.
16. Korkegi, Robert H.: Transition Studies and Skin-Friction Measurements on an Insulated Flat Plate at a Mach Number of 5.8. J. Aeron. Sci., vol. 23, no. 2, Feb. 1956, pp. 97-107, 192.

TABLE I. — SPECIFICATIONS OF SKIN-FRICTION GAGE



Range, full scale, grams/centimeter ²	0 to ±1, 0 to ±3
Output signal at full scale, volts	±5
Output impedance, maximum, ohms	5000
Linearity deviation, percent of full scale	0.3
Natural frequency, minimum cycles per second	150
Null stability, percent of full scale —	
At 70° F (21° C)	0.5
At 70° F (21° C) to 212° F (100° C)	1
Temperature, ° F (° C) —	
Without cooling	-40 to 212 (-40 to 100)
With water jacket	-40 to 1500 (-40 to 816)
Linear-acceleration sensitivity, percent full scale per g	1
Overload, grams/centimeter ²	100
Input voltage, volts	28
Input current, milliamperes	40
Resolution, grams/centimeter ²	0.0001
Output signal isolation from power ground and case, megohms	1
Area of floating element, foot ² (centimeter ²).	7.629×10^{-4} (0.7088)

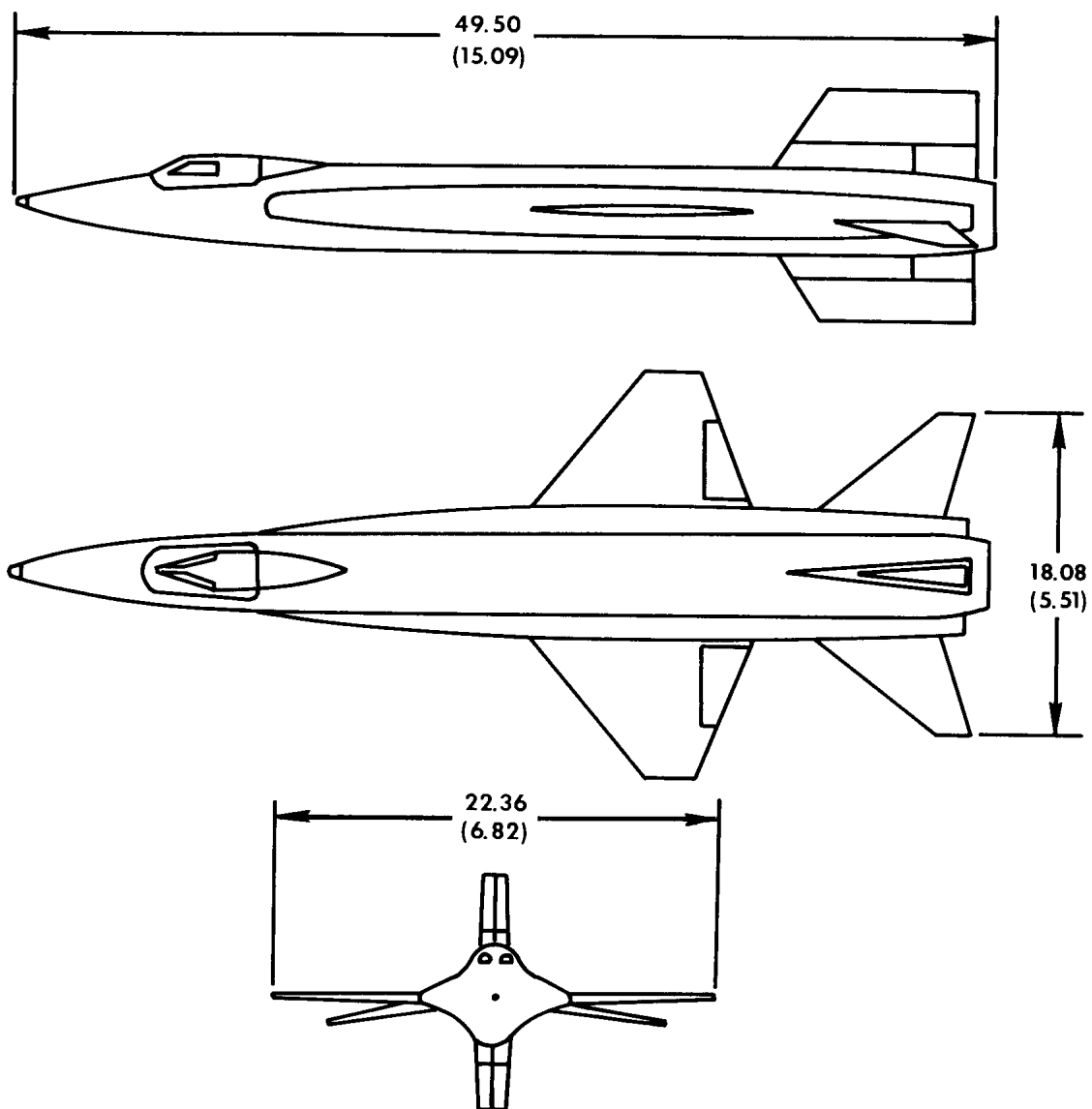
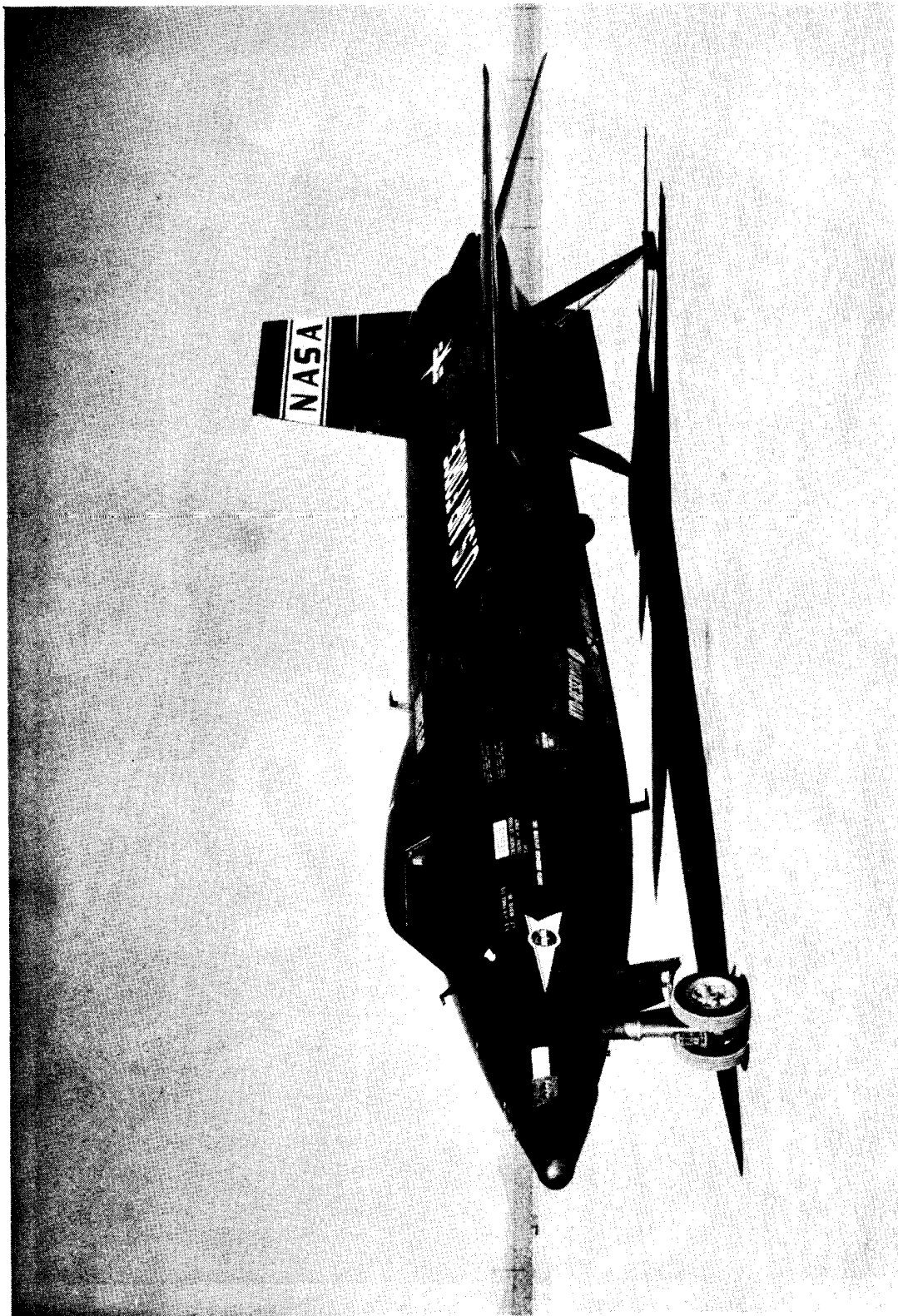


Figure 1. – Three-view drawing of the X-15, with the blunt leading edge vertical fin.
Dimensions in feet (meters).



E-7902

Figure 2. - X-15 airplane with the blunt-leading-edge vertical fin.



Figure 3. — Closeup of X-15 upper vertical fin with sharp leading edge.

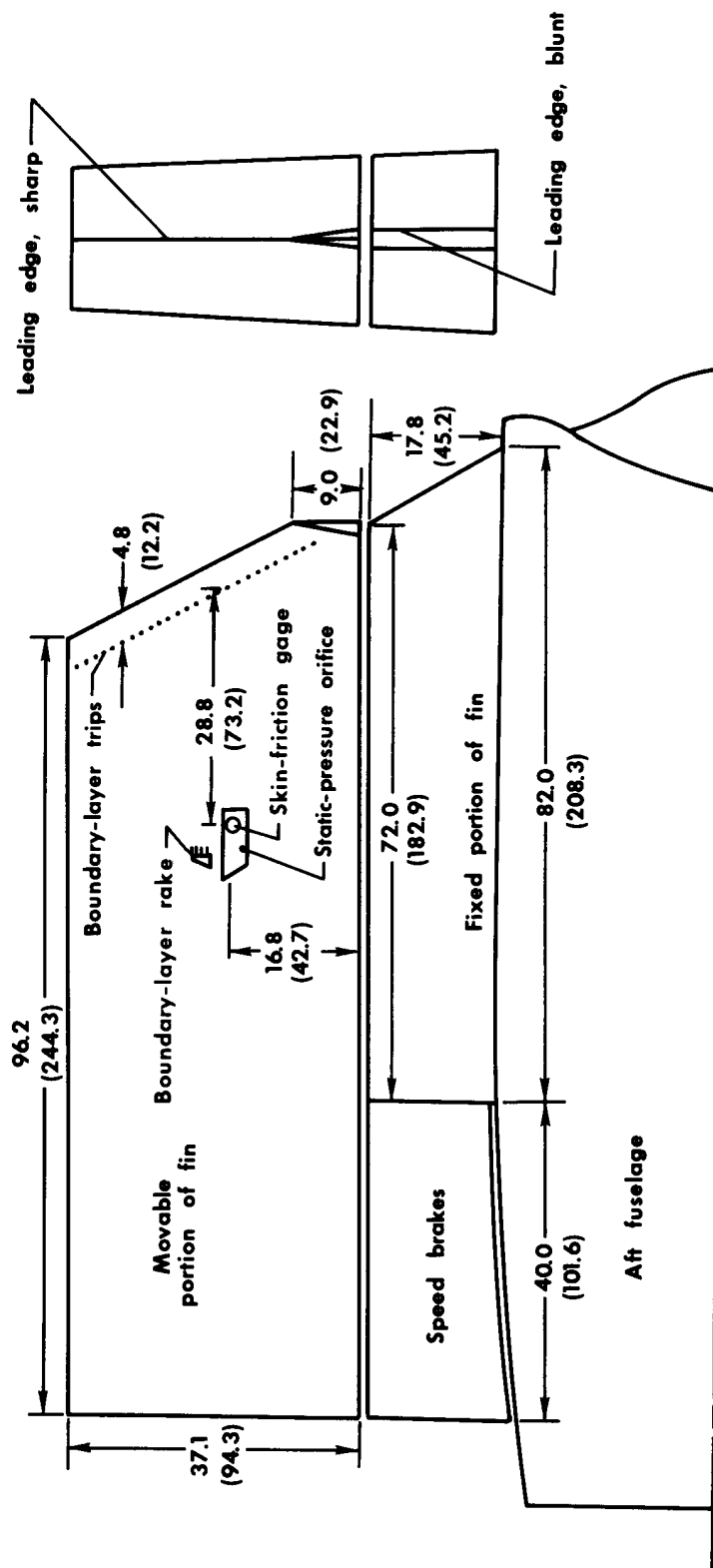
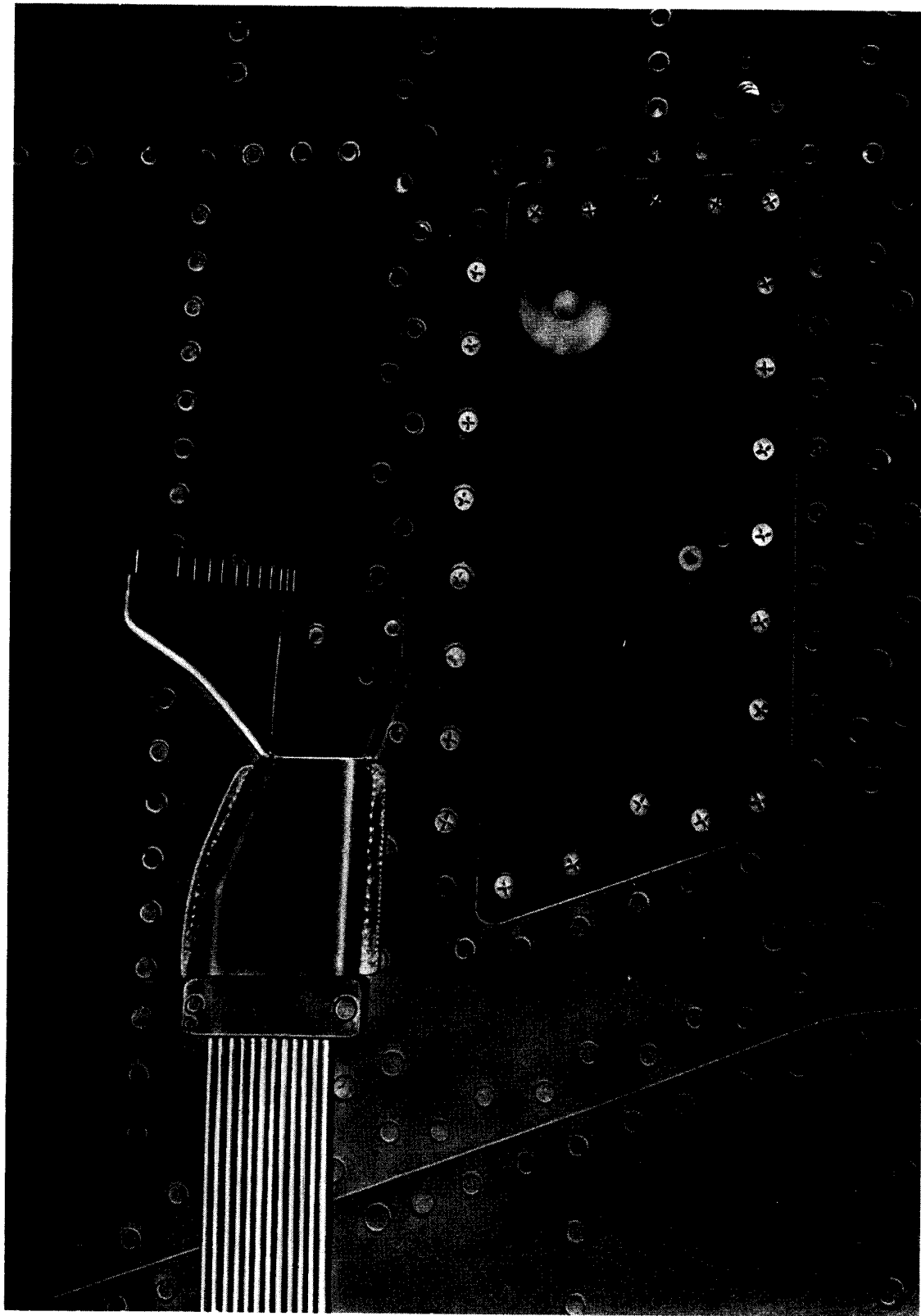
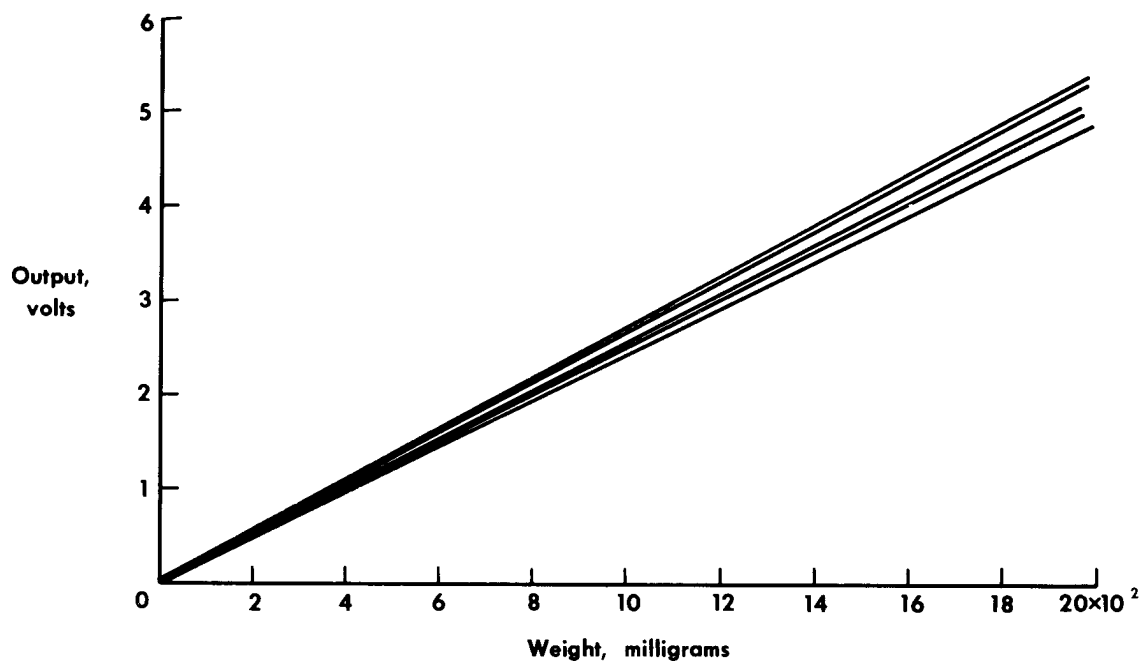


Figure 4. - Sketch of vertical fin with sharp leading edge showing location of test panel (not drawn to scale). Dimensions in inches (centimeters).

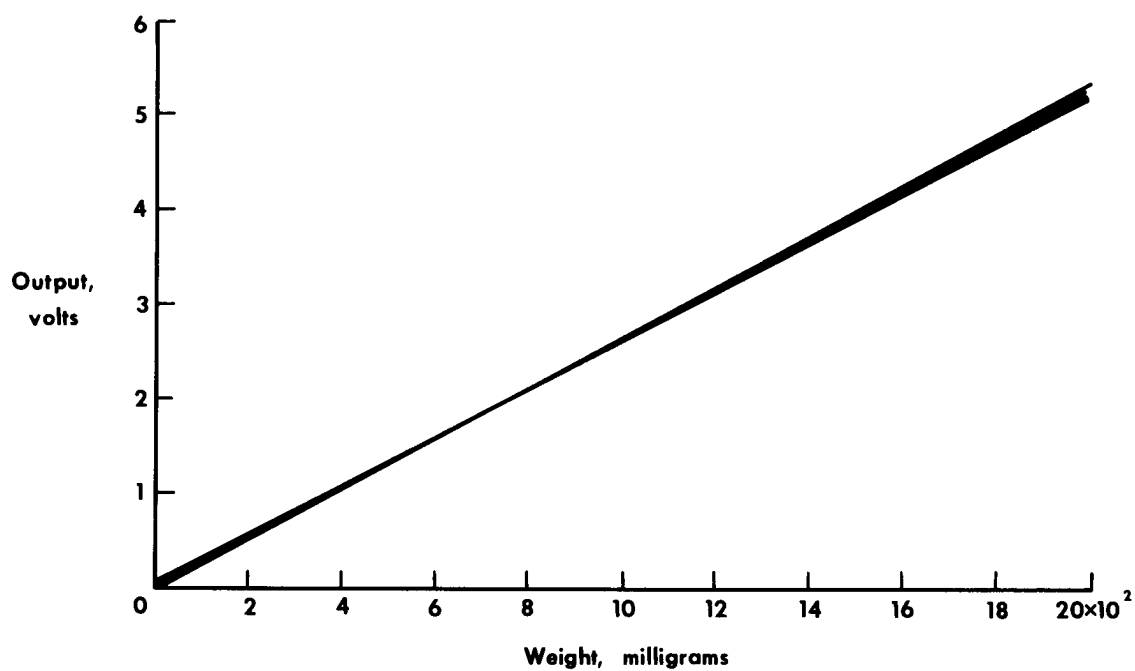


E-16041

Figure 5. - Closeup view of installation before heads of screws in front of skin-friction gage were filled and ground.

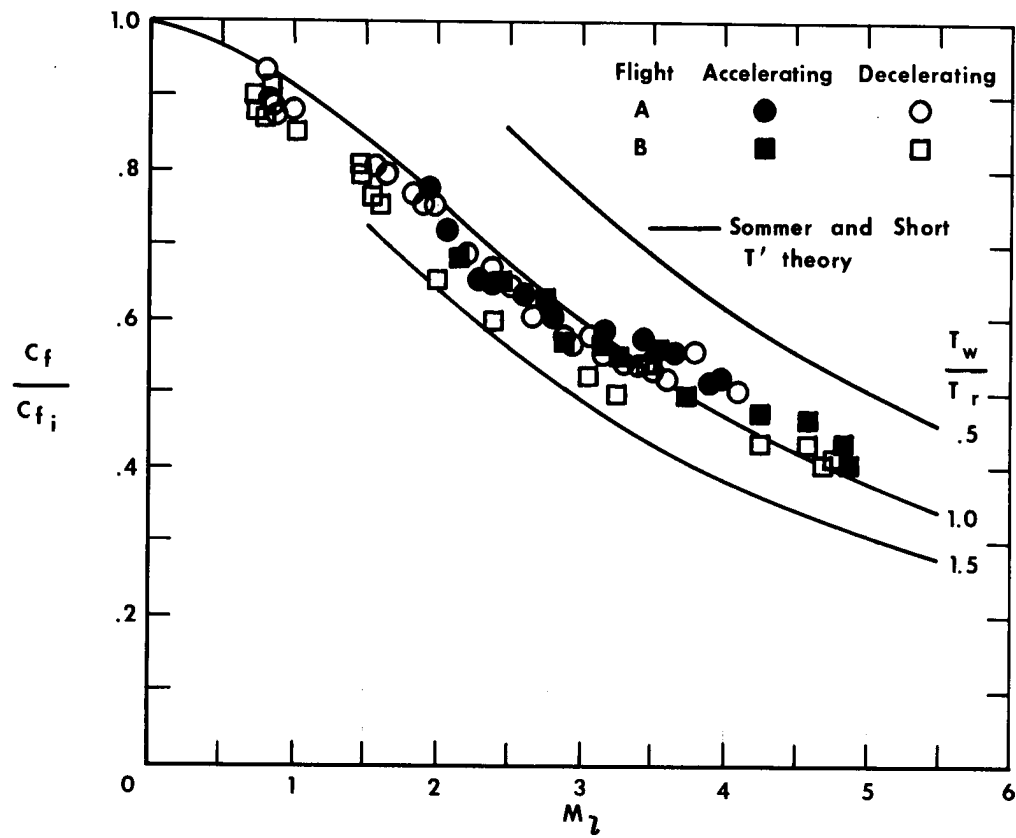


(a) Before transient-temperature tests.

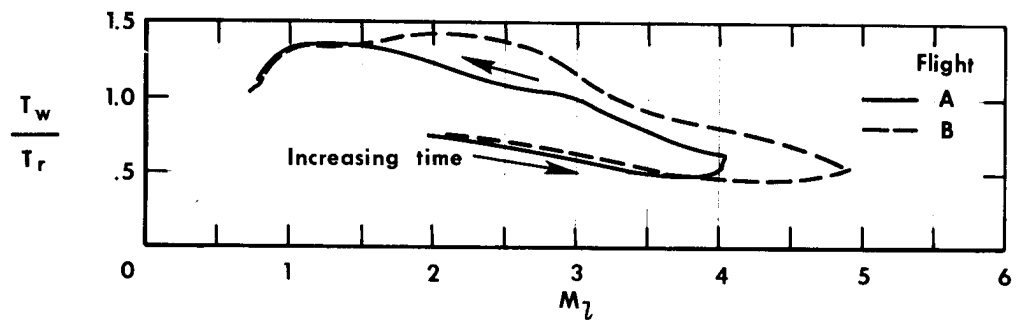


(b) After transient tests.

Figure 6. — Calibration of skin-friction gage for each of several constant-temperature values. $-70^{\circ}\text{ F} < T < 200^{\circ}\text{ F}$ ($-57^{\circ}\text{ C} < T < 93^{\circ}\text{ C}$).



(a) Variation of the ratio $\frac{C_f}{C_{f_i}}$ with local Mach number.



(b) Variation of the ratio $\frac{T_w}{T_r}$ with local Mach number.

Figure 7. — Comparison of flight-determined skin-friction coefficients with the T' method of Sommer and Short, for a varying wall-to-recovery temperature ratio.

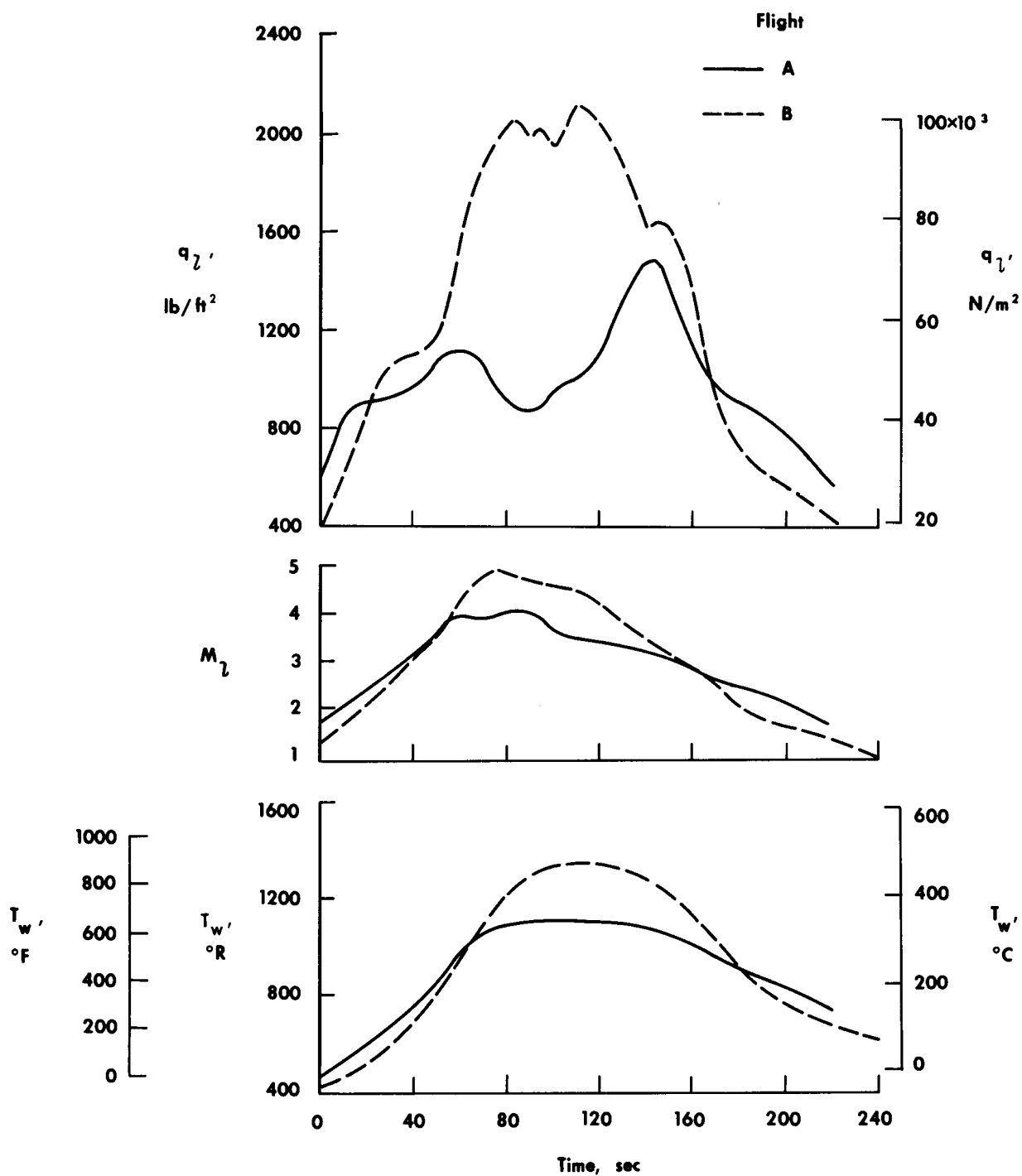


Figure 8.— History of significant local parameters.

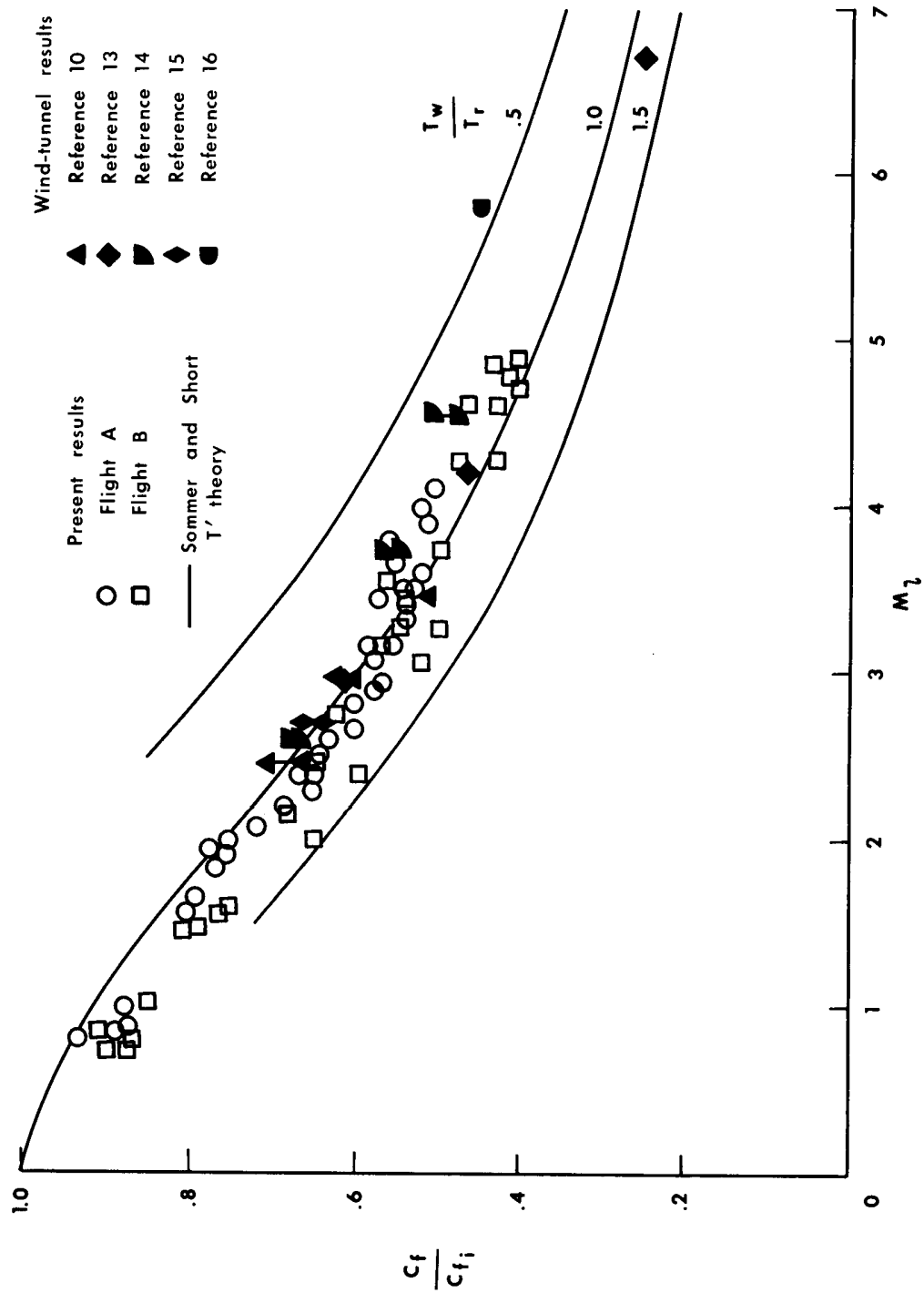


Figure 9. -- Comparison of flight results with wind-tunnel experiments and theory.

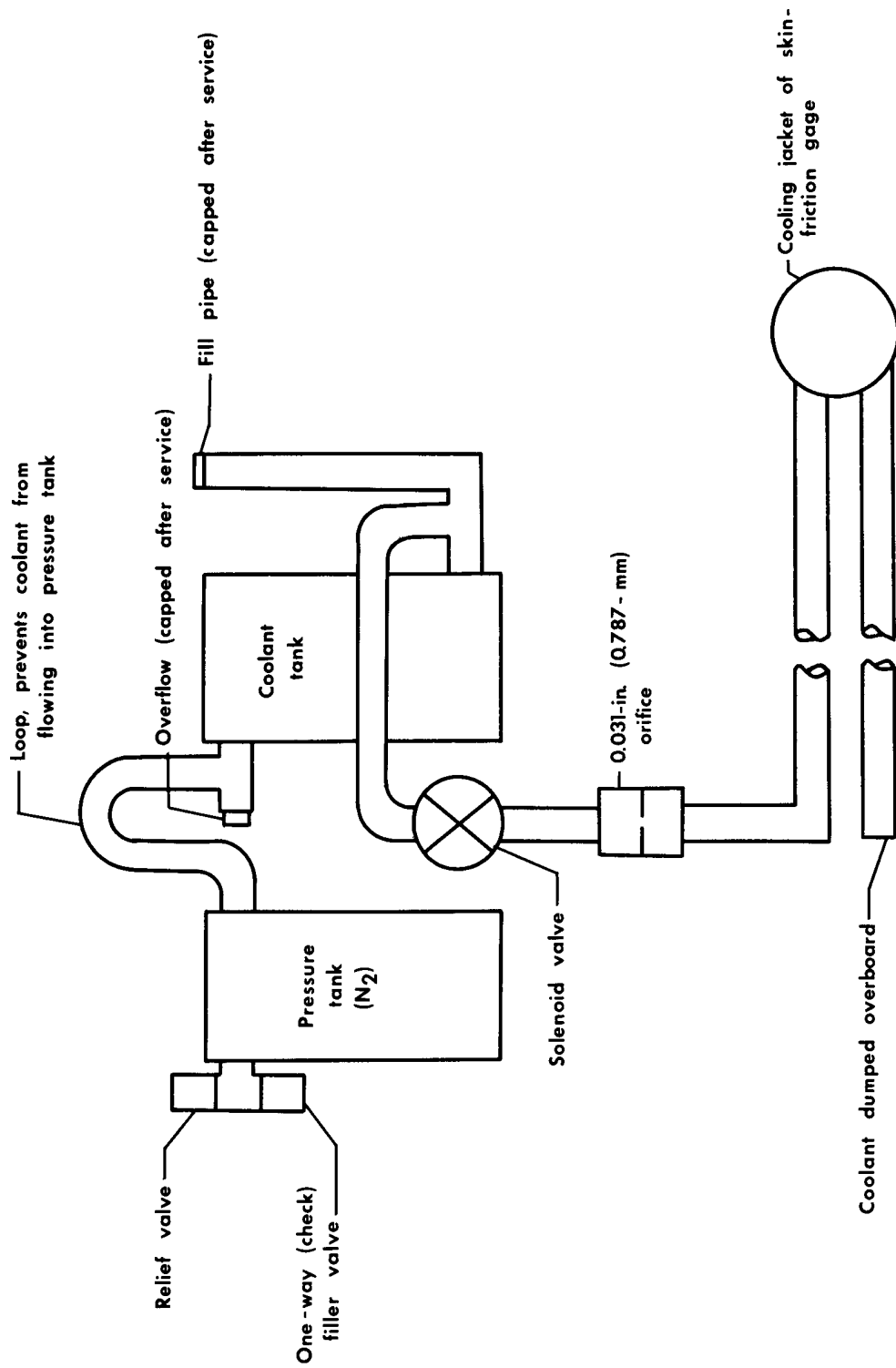
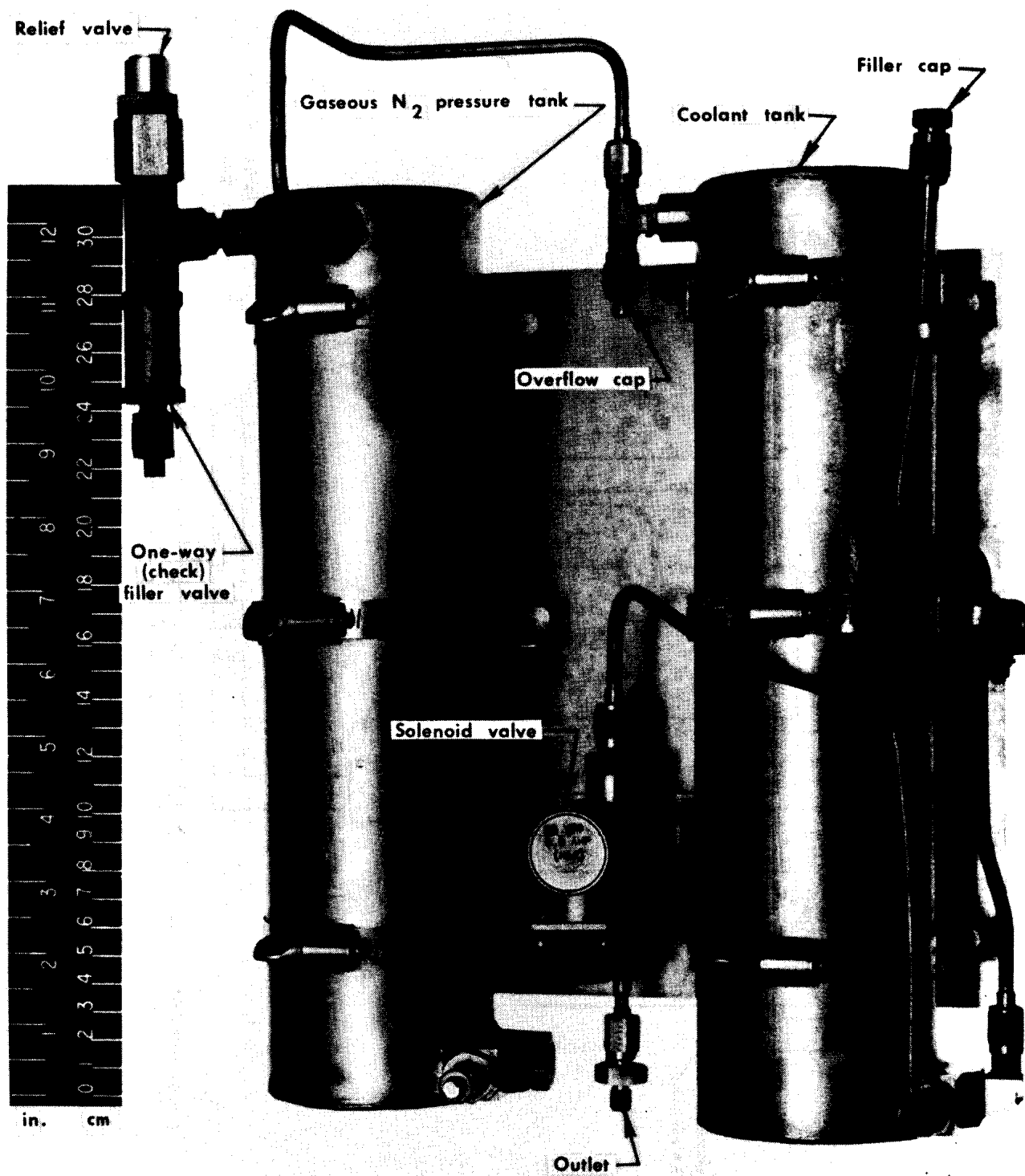
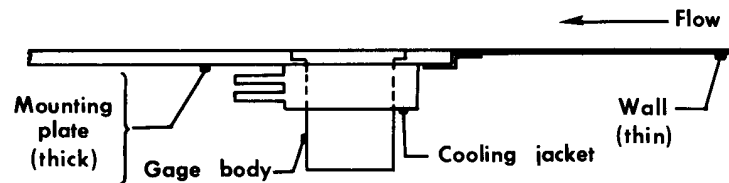


Figure 10. — Schematic drawing of cooling system.

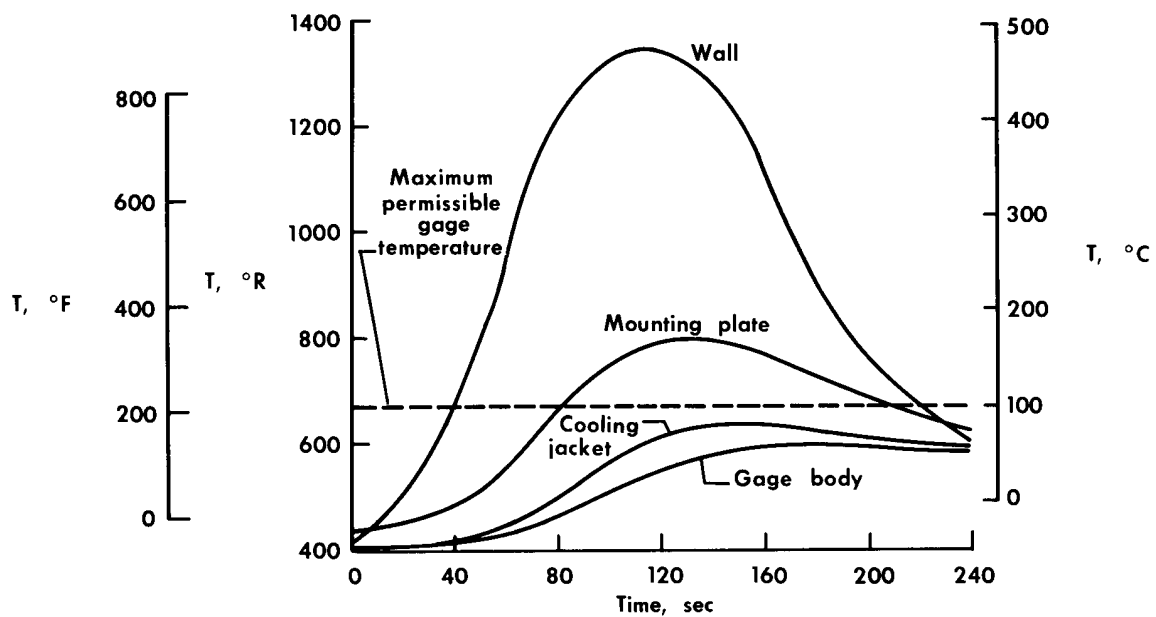


E-14796

Figure 11. - Pressure tank, coolant tank, valves, and other connecting parts of the cooling system.



(a) Location of thermocouples.



(b) History of temperature.

Figure 12. - Variation of temperature with time at selected locations.